



引文格式: 王文宝, 李卫星, 雷聪聪, 等. 中亚造山带中段早—中三叠世埃达克岩和 A 型花岗岩成因及构造意义[J]. 西北地质, 2024, 57(3): 29–43. DOI: 10.12401/j.nwg.2023114

Citation: WANG Wenbao, LI Weixing, LEI Congcong, et al. Early-Middle Triassic Adakitic and A-type Granite in Middle Segment of Central Asian Orogenic Belt: Petrogenesis and Tectonic Implications[J]. Northwestern Geology, 2024, 57(3): 29–43. DOI: 10.12401/j.nwg.2023114

中亚造山带中段早—中三叠世埃达克岩和 A 型花岗岩成因及构造意义

王文宝^{1,*}, 李卫星^{1,*}, 雷聪聪¹, 马军¹, 闫振军¹, 薄海军¹, 丁海生¹, 彭渊哲²

(1. 中国地质调查局呼和浩特自然资源综合调查中心, 内蒙古 呼和浩特 010020;

2. 陕西矿业开发工贸有限公司, 陕西 西安 710054)

摘要: 中亚造山带增生过程中发育的典型岩浆作用是研究其演化过程的关键。中亚造山带中段南缘达伦乌苏二长花岗岩、花岗斑岩系统的岩石学、地球化学和年代学研究表明, 达伦乌苏二长花岗岩具有明显高 Sr、低 Y、Yb 含量, 高 Sr/Y 值 (88.55~140.34), 无明显 Eu 异常 (δEu 值为 0.68~0.98), 具埃达克岩地球化学特征。花岗斑岩富 SiO_2 , 贫 CaO 和 MgO , 具高的 $\text{FeO}/(\text{FeO}+\text{MgO})$ 和 $10\,000\times\text{Ga/Al}$ 值, 高 Zr 、 Nb 、 Ta 含量, 富集 Pb 、 Hf 、 Rb 、 K 和 Th , 相对亏损 Ba 、 Sr 、 P 和 Ti , 属于典型的 A 型花岗岩。二者的锆石 U-Pb 年龄分别为 $(249.0\pm2.3)\text{ Ma}$ 和 $(241.0\pm2.8)\text{ Ma}$ 。结合区域地质资料, 埃达克岩指示了古亚洲洋闭合后陆壳碰撞加厚的背景, 而 A 型花岗岩指示了碰撞后伸展构造背景。两种典型的岩浆作用记录了早—中三叠世中亚造山带中段南缘由增生造山到造山后期伸展的转换过程。

关键词: 中亚造山带; 锆石 U-Pb 年龄; 三叠纪; 埃达克岩; A 型花岗岩; 阿拉善

中图分类号: P588.12

文献标志码: A

文章编号: 1009-6248(2024)03-0029-15

Early-Middle Triassic Adakitic and A-type Granite in Middle Segment of Central Asian Orogenic Belt: Petrogenesis and Tectonic Implications

WANG Wenbao¹, LI Weixing^{1,*}, LEI Congcong¹, MA Jun¹, YAN Zhenjun¹,
BO Haijun¹, DING Haisheng¹, PENG Yuanzhe²

(1. Hohhot General Survey of Natural Resources Center, China Geological Survey, Hohhot 010020, Inner Mongolia, China;

2. Shaanxi Mining Industry and Trade Co., Ltd., Xi'an 710054, Shaanxi, China)

Abstract: Typical igneous rocks during the accretionary orogeny process in the Central Asian Orogenic Belt (CAOB) play a key role in understanding its tectonic evolution. We present new LA-ICP-MS in-situ zircon U-Pb and bulk geochemical data for the Dalunwusu monzogranite and granite porphyry suites which are located in

收稿日期: 2022-12-03; 修回日期: 2023-06-11; 责任编辑: 曹佰迪

基金项目: 中国地质调查局项目“内蒙古自治区额济纳旗辉森乌拉等三幅 1:5 万区域地质调查”(DD20230252), “内蒙古自治区额济纳旗克克桃勒盖等 4 幅区域地质调查”(ZD20220503)联合资助。

作者简介: 王文宝(1989-), 男, 工程师, 从事区域地质调查工作。E-mail: wangwenbao1989@163.com。

* 通讯作者: 李卫星(1990-), 男, 工程师, 从事区域地质调查工作。E-mail: 1025992795@qq.com。

Southernmost CAOB. The Dalunwusu monzogranites, have a crystallization age of (249.0 ± 2.3) Ma, exhibit adakite-like geochemical characteristics, such as high Sr content and low Yb and Y contents, coupled with high Sr/Y values ($88.55\sim140.34$) and show a weakly negative Eu anomalies ($\delta\text{Eu}=0.68\sim0.98$). Geochemical compositions indicate the Dalunwusu monzogranites derived from partial melting of mafic granulite in the lower thickened crust. The Dalunwusu granite porphyry, have a crystallization age of (241.0 ± 2.8) Ma, show typical geochemical features of A-type granites, which are characterized by having high SiO_2 , low CaO and MgO content, high $\text{FeO}_{\text{v}}/(\text{FeO}_{\text{v}}+\text{MgO})$ and $10\,000\times\text{Ga}/\text{Al}$ values. Moreover, the granite porphyry show trace element features of A-type granites including rich in Zr, Nb, Ta abundances, and high values for Pb, Hf, Rb, K and Th, and low values for Ba, Sr, P, and Ti. Taking into account available data of the regional geological background, we may suggest that the adakites were products through partial melting of the thickened lower crust after the closure of the Paleo-Asian Ocean, and the A-type granite porphyry were likely produced at the tectonic setting of post-collisional phase with crustal extension and thinning. These two typical igneous rocks reflect the shift of geodynamic setting, from an earlier accretionary orogen environment to a later extensional setting during early-middle Triassic.

Keywords: central Asian Orogenic belt; zircon U-Pb age; triassic; adakite; A-type granite; Alxa

中亚造山带横亘于西伯利亚板块和华北-塔里木板块之间,其形成与古亚洲洋及其陆缘的演化密切相关([Şengör et al., 1993](#); [Badarch et al., 2002](#); [Xiao et al., 2003, 2018](#); [Windley et al., 2007](#); [付超等, 2023](#); [张永玲等, 2024](#))。关于古亚洲洋或其分支洋闭合时限存在泥盆纪—早石炭世([Charvet et al., 2007](#); [Xu et al., 2013](#); [邵济安等, 2014](#); [刘桂萍等, 2021](#))和二叠纪至早—中三叠世不同认识([Xiao et al., 2003, 2018](#); [Li, 2006](#); [Windley et al., 2007](#); [Jian et al., 2008](#); [Zheng et al., 2020, 2021](#)),究其原因,可能与古亚洲洋自西向东剪刀式闭合有关或多期造山有关([Wang et al., 2022](#); [Li et al., 2022](#)),且西伯利亚板块与华北-塔里木板块之间存在不同时期的微陆块和岛弧,不同地体碰撞拼贴的时间也存在差异([陈井胜等, 2022](#); [董玉等, 2022](#))。中亚造山带各个部分地质演化记录的研究能够丰富对其构造演化过程的精细认识。

内蒙古阿拉善盟额济纳旗位于中亚造山带中段南缘,是连接造山带东、西两段的关键部位,区域出露有大量岩浆岩,记录了深部壳幔相互作用的信息,是研究中亚造山带构造演化过程的关键。埃达克岩被认为形成于“高压”构造环境([张旗等, 2002, 2003, 2020](#)),有学者将埃达克岩的产出作为中亚造山带处于俯冲/碰撞期的标志([谢春林等, 2009](#); [Li et al., 2012, 2013, 2017](#); [Liu et al., 2012](#); [Liu et al., 2019](#); [Lu et al., 2020](#); [Wang et al., 2020](#); [Zheng et al., 2020, 2021](#); [Luan et al., 2022](#))。A型花岗岩被认为形成于伸展的构造环

境([Eby, 1992](#)),A型花岗岩的侵位时代可限定其造山后伸展作用的时限([Wu et al., 2002](#); [Shi et al., 2004](#); [Li et al., 2012](#); [Shi et al., 2016](#); [Zheng et al., 2016](#); [Du et al., 2018](#); [Eizenhöfer et al., 2018](#); [Lu et al., 2020](#); [Song et al., 2020](#)),这些包括埃达克岩和A型花岗岩在内的典型岩浆作用可为理解中亚造山带洋陆演化过程提供关键约束([王元元等, 2023](#); [舍建忠等, 2023](#))。

区域地质调查工作过程中在内蒙古阿拉善盟额济纳旗达伦乌苏地区新识别出了两期岩浆岩,利用岩石学、同位素地质年代学和岩石地球化学研究方法,确定了其活动时代,探讨了其成因和构造背景,为该区域典型岩浆作用和构造演化史的研究提供了新证据。

1 区域地质背景与岩石学特征

1.1 区域地质背景

研究区南侧恩格尔乌苏蛇绿混杂岩带内见有超镁铁岩、辉长岩、枕状和块状玄武岩、硅质岩、细碧岩等,其中辉长岩锆石U-Pb年龄为380 Ma([王廷印等, 1993](#)),枕状玄武岩显示正常型大洋中脊玄武岩特征,其SHRIMP锆石U-Pb年龄为 (302 ± 14) Ma([Zheng et al., 2014](#)),多被认为是古亚洲洋在本段的最终闭合位置,向东与索伦蛇绿岩带相连,该蛇绿混杂岩带以北属中亚造山带的中段。研究区北侧蒙古境内Gurvan Sayhan-Zoolen蛇绿岩带的蛇绿岩组分形成于520~511

Ma, 被(494±6)Ma的闪长岩脉截切侵入, 代表了北侧 Zoolen 洋和对接带(Jian et al., 2014)。雅干断裂带近 EW 向横穿研究区, 两侧古生代地层、火山岩和侵入岩特征存在明显差异, 长期以来被视为一条重要的地质界线, 北侧主体为奥陶纪—石炭纪岛弧, 南侧为珠斯楞-杭乌拉大陆边缘(吴泰然等, 1993; 王廷印等, 1993; Windley et al., 2007; 郑荣国等, 2013; Liu et al.,

2016, 2017, 2018)。研究区向西与北山造山带隔巴丹吉林沙漠相望, 向东雅干断裂带所分隔的两地体分别与 Badarch 等(2002)在蒙古境内划分具岛弧性质的 Hashaat 地体和具克拉通性质的南戈壁微陆块相连(图 1a)。达伦乌苏二长花岗岩、花岗斑岩紧邻雅干断裂带, 位于其北侧, 侵入石炭系地层和更早期的岩体中(图 1a、图 1b)。

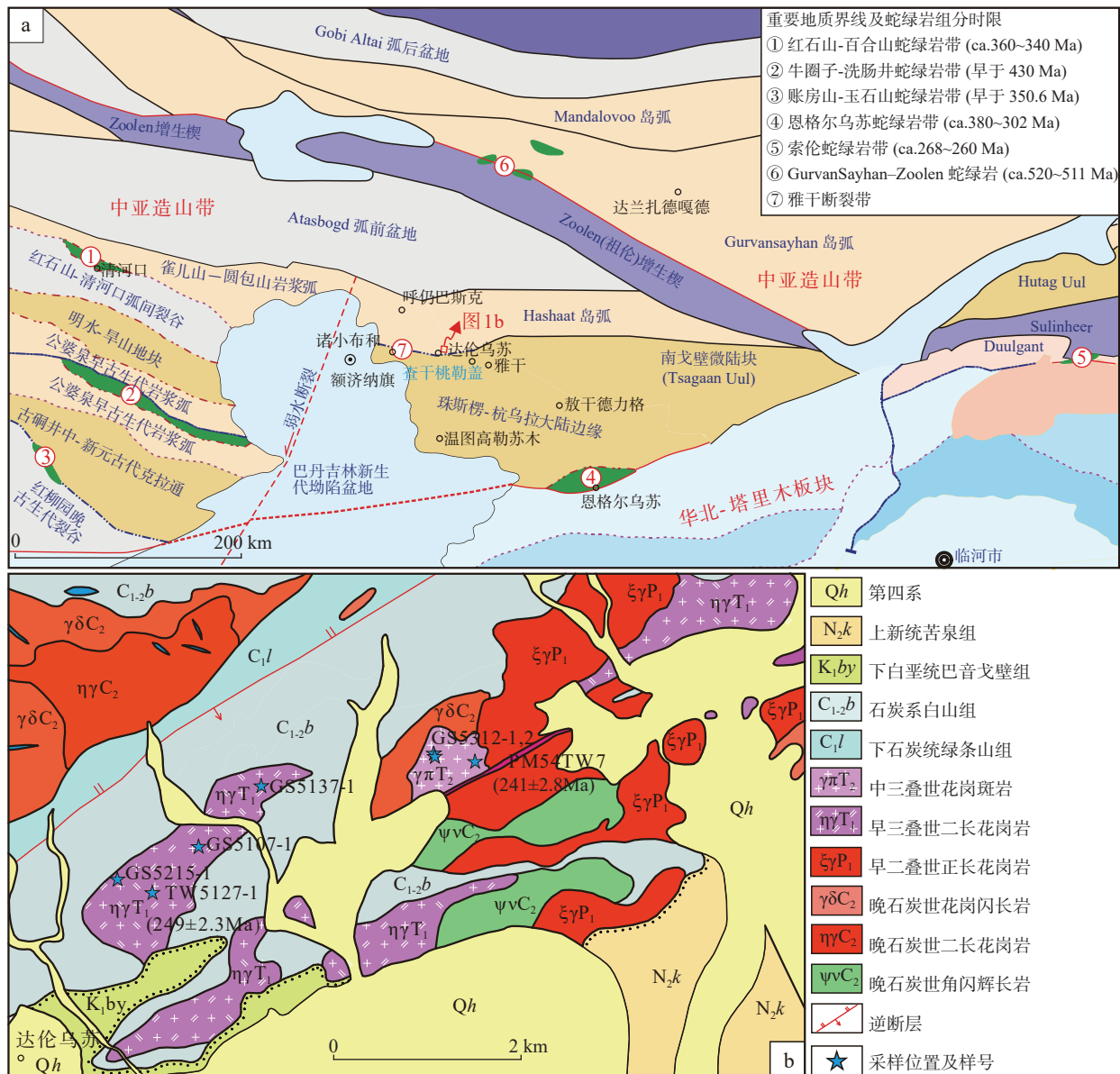


图 1a 据吴泰然等(1993)、Badarch 等(2002)、邵积东(2016)和辛后田等(2020)修; 蛇绿岩时限据 Zheng 等(2014)、Jian 等(2014)、Fu 等(2018)和辛后田等(2020)

图 1 内蒙古西部大地构造简图(a)及研究区地质简图(b)

Fig. 1 (a) Tectonic map of the western Inner Mongolia and (b) sketch geological map of the study area

1.2 岩石学特征

达伦乌苏早三叠世二长花岗岩体北东向展布,

出露面积约为 3.2 km², 侵入石炭系白山组和早期角闪辉长岩中, 局部被下白垩统巴音戈壁组和第四系

冲洪积物不整合覆盖(图1b)。岩石多为似斑状花岗结构。斑晶主要为钾长石,大者可达3 cm,含量约为5%~10%。基质为中粗粒花岗结构,矿物大小

多为3~10 mm,主要由斜长石(35%~40%)、钾长石(20%~25%)、石英(30%)和少量黑云母组成(图2a、图2b)。



Pl. 斜长石; Kfs. 钾长石; Bt. 黑云母; Qtz. 石英

图2 达伦乌苏早三叠世二长花岗岩(a、b)和中三叠世花岗斑岩岩体(c、d)野外及镜下特征

Fig. 2 (a, b) Representative photomicrographs of the Dalunwusu early-middle Triassic monzogranite and (c, d) granite porphyry

达伦乌苏中三叠世花岗斑岩呈一小岩株产出,出露面积约0.5 km²,侵入早二叠世正长花岗岩和晚石炭世花岗闪长岩中,局部被第四系冲洪积物覆盖(图1b)。岩石呈斑状-似斑状结构,多由斑晶和基质组成。斑晶见斜长石、钾长石及石英,粒径0.2~2.5 mm不等。斜长石呈半自形板状,镜下隐约可见聚片双晶,部分可见环带构造。钾长石为(正)条纹长石,呈半自形板状,部分粒内嵌布板条状斜长石。石英呈他形粒状,多聚集在一起分布。基质由微细粒的长石、石英及少量白云母组成(图2c、图2d)。岩体整体钼含量较高,其中曾发现了多条钼矿体。

2 样品采集和分析测试方法

本次研究在额济纳旗达伦乌苏北早三叠世二长花岗和中三叠世花岗斑岩内各采集了一件锆石U-Pb

同位素测年样品,具体采样位置见图1b。样品采自新鲜的岩石露头,粗碎清洗剔除风成砂和风化面。锆石分选、制靶、阴极发光(CL)照相和LA-ICP-MS锆石U-Pb同位素分析均在中国冶金地质总局山东局测试中心完成。锆石U-Pb同位素测试使用美国Coherent公司生产的193nmArF准分子系统,ICP-MS为美国热电Thermo iCAP Q,激光束斑直径为30 μm,激光脉冲10 Hz。测试采用标准锆石91500作为外部标准物质,元素含量采用NIST610作为外标,²⁹Si作为内标元素,具体实验测试方法与李凤春等(2016)相同。样品的同位素比值及元素含量计算采用ICPMSCAL程序,普通铅校正采用ComPbCorr#3.17校正程序,U-Pb谐和图和年龄权重平均计算采用Isoplot程序(Ludwig, 2003)完成。

在岩体的不同位置采集了主、微量元素和稀土元素测试样品。其中二长花岗岩4件(GS5215-1、GS5137-1、

GS5107-1、TW5127-1), 花岗斑岩3件(PM54TW7、GS5312-1、GS5312-2), 具体采样位置见图1b。样品主量元素测试工作采用X射线荧光法进行分析(XRF), 在中国地质调查局呼和浩特自然资源综合调查中心实验室 Axios MaxX-荧光光谱仪上完成。稀土、微量元素分析测试工作在中国冶金地质总局山东局测试中心完成, 其中Cs、Ba、Nb、Rb、Zr元素分析采用X荧光光谱法分析, 其他元素在X Series2电感耦合等离子体质谱仪(YQ006)上完成, 具体分析流程与Yan等(2019)相同。

3 分析测试结果

3.1 锆石U-Pb测年

TW5127-1样品锆石多为自形短柱状晶体, 其长轴多为130~220 μm, 长宽比在1.5~2.5之间, 阴极发光图像显示锆石显示有清晰的震荡环带, 具岩浆锆石特征(图3a)。除去部分锆石普通铅过高和未获有效的平坦的波谱段外, 样品中的23个测点具相近的单颗粒锆石年龄, 详细分析结果见表1。锆石Th含量为 $240.0 \times 10^{-6} \sim 935.0 \times 10^{-6}$, U含量为 $545.8 \times 10^{-6} \sim 1250.5 \times 10^{-6}$, Th/U值为0.39~0.91(均>0.1), 锆石 $^{206}\text{Pb}/^{238}\text{U}$ 年龄为240~257 Ma, 23个点测试结果均位于谐和线附近, 其 $^{206}\text{Pb}/^{238}\text{U}$ 加权平均年龄为(249.0±2.3)Ma(MSWD=3.4, n=23)(图4a、图4b), 代表了该二长花岗岩的结晶年龄。

PM54TW7样品锆石多为自形长柱状晶体, 其长轴为250~500 μm, 长宽比为2.5~5.5, 阴极发光图像

显示锆石具有清晰的震荡环带, 为岩浆锆石(图3b)。除去部分测点普通铅过高和未获有效的平坦的波谱段外, 样品中的14个锆石获得了较谐和的单颗粒锆石年龄, 详细分析结果见表1。其Th含量为 $284.9 \times 10^{-6} \sim 786.6 \times 10^{-6}$, U含量为 $523.6 \times 10^{-6} \sim 1085.9 \times 10^{-6}$, Th/U值为0.54~0.95(均>0.1), 显示岩浆成因锆石特征。锆石 $^{206}\text{Pb}/^{238}\text{U}$ 年龄为232~249 Ma, 14个点测试结果均位于谐和线附近, 其 $^{206}\text{Pb}/^{238}\text{U}$ 加权平均年龄为(241.0±2.8) Ma (MSWD=1.9, n=14), 代表了该花岗斑岩的结晶年龄(图4c、图4d)。

3.2 主、微量元素测试结果

达伦乌苏早三叠世浅肉红色二长花岗岩和中三叠世紫红色花岗斑岩主、微量元素分析结果见表2。

达伦乌苏早二叠世二长花岗岩样品SiO₂含量为71.21%~72.71%, 平均含量为71.87%, 在TAS分类图解中样品落入花岗岩区(图5a)。样品全碱含量高($\text{K}_2\text{O}+\text{Na}_2\text{O}=7.72\% \sim 8.29\%$), $\text{Na}_2\text{O}/\text{K}_2\text{O}=0.73 \sim 1.19$, 平均为0.96, 属高钾钙碱性系列(图5b、图5c)。其Al₂O₃含量为14.84%~15.12%, 平均为15%, A/CNK值均>1且<1.1(1.03~1.10), 在A/NK-A/CNK图解中样品全部落入过铝质区域内(图5c)。样品Sr含量较高, 在 $395 \times 10^{-6} \sim 748 \times 10^{-6}$ 之间, 平均含量为 508×10^{-6} ($>400 \times 10^{-6}$)。具有较低的Y($4.10 \times 10^{-6} \sim 5.33 \times 10^{-6}$, 平均 $<18 \times 10^{-6}$)和Yb($0.36 \times 10^{-6} \sim 0.47 \times 10^{-6}$, 平均 $<1.9 \times 10^{-6}$)含量。具较高的Sr/Y值(88.55~140.34, >20~40)。在球粒陨石标准化图解中稀土配分曲线呈右倾型, 富集轻稀土元素而亏损重稀土元素, 样品无明显Eu异常, δEu值为0.68~0.98, 平均为0.89(图6a)。

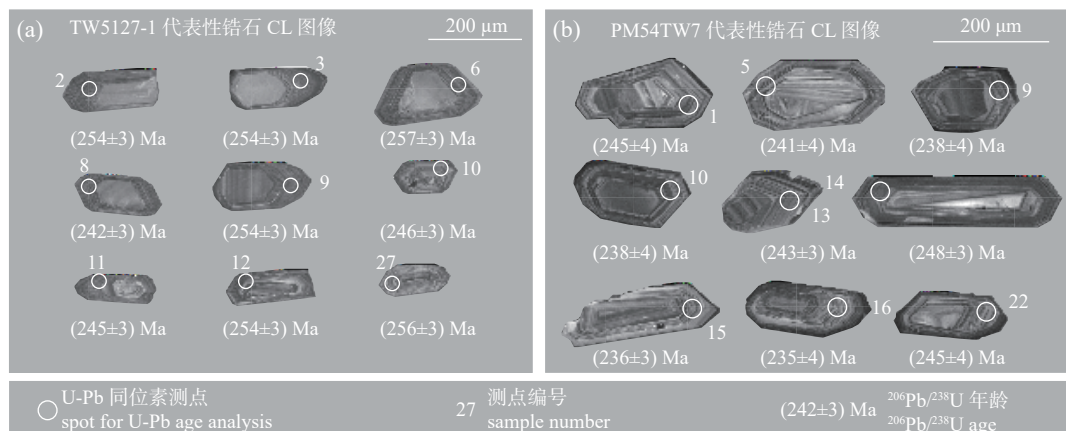


图3 达伦乌苏二长花岗岩(a)和紫红色花岗斑岩体(b)代表性锆石阴极发光图像

Fig. 3 (a) The cathodoluminescence (CL) images of typical zircon grains of the Dalunwusu early- middle Triassic monzogranite and (b) granite porphyry

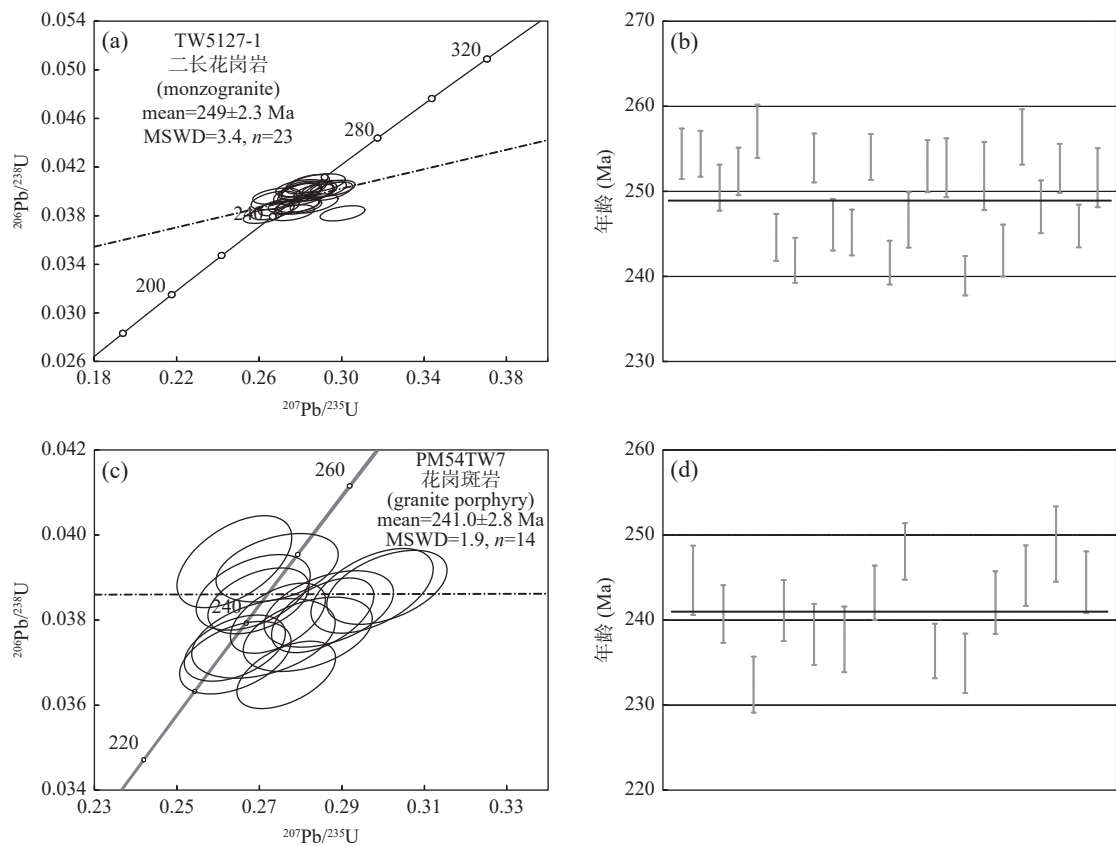


图4 达伦乌苏二长花岗岩(a、b)和紫红色花岗斑岩体(c、d)锆石U-Pb年龄谐和图

Fig. 4 (a, b) LA-ICP-MS U-Pb zircon concordia diagram of the Dalunwusu early-middle Triassic monzogranite and (c, d) granite porphyry

在微量元素蛛网图中, 岩体明显富集 Sr、K、Th、Rb, 相对亏损 Nb、Ta、P、Ti(图 6b)。

达伦乌苏中三叠世花岗斑岩样品 SiO_2 含量为 77.00%~78.08%, 平均为 77.44%, 在 TAS 分类图解中样品落入花岗岩区(图 4a)。岩石富碱, $(\text{Na}_2\text{O}+\text{K}_2\text{O})$ 含量为 7.93%~8.27%, 平均为 8.10%; $\text{K}_2\text{O}/\text{Na}_2\text{O}$ 为 0.38~0.62, 属高钾钙碱性系列(图 4b、图 4c)。样品具有较低的 CaO 含量为 0.54%~0.72% 和 Al_2O_3 含量为 11.35%~12.27%, 平均为 11.74%, 其 A/CNK 值接近 1(1.02~1.05), 属过铝质岩石(图 4d)。样品 MgO 含量较低 0.14%~0.19%, $\text{Mg}^{\#}$ 值亦较低, 介于 15.34~17.69(表 2)。稀土总量较低 36.59×10^{-6} ~ 43.83×10^{-6} , 轻重稀土分馏明显($\text{LREE}/\text{HREE}=8.33 \sim 12.34$, $(\text{La}/\text{Yb})_{\text{N}}=6.86 \sim 11.44$), 轻稀土内部分馏亦明显($\text{La}/\text{Sm}_{\text{N}}=7.90 \sim 11.11$), 重稀土元素相对平坦, 具中等 Eu 负异常($\delta\text{Eu}=0.38 \sim 0.64$), 稀土元素球粒陨石标准化图解中配分曲线呈“右倾海鸥型”(图 6a)。在微量元素蛛网图中, 样品明显富集高场强元素 Th、U、Rb、K, 相

对亏损 Ba、Sr、P、Ti(图 6b)。样品 $10\,000 \times \text{Ga}/\text{Al}$ 值为 2.80~3.31(均大于 2.6)。

4 讨论

4.1 岩体的年代学意义

笔者获得的锆石 U-Pb 年龄显示达伦乌苏二长花岗岩、花岗斑岩岩体分别形成于 (249.0 ± 2.3) Ma、 (241.0 ± 2.8) Ma, 侵位于早—中三叠世。该年龄修正了雅干幅 1:20 万区域地质矿产调查中在达伦乌苏二长花岗岩体的长石中获得的 K-Ar 年龄为 193.5 Ma。区域三叠系分布较少, 目前已知的仅在苏亥特高勒南东、拐子湖附近零星出露上三叠统珊瑚井组。前人在研究区西具低 Sr/Y 值的乔伦恩格次岩体获得了 (236.8 ± 2.1) Ma 的锆石 U-Pb 年龄(王丕军, 2018; 刘基等, 2020), 望湖山岩体获得了 230 Ma 的锆石 U-Pb 年龄(Liu et al., 2018)。达伦乌苏两期岩体是区域三叠纪岩浆作用和区域地质演化研究的新载体。

表2 达伦乌苏早三叠世二长花岗岩和中三叠世花岗斑岩主、微量元素分析测试结果

Tab. 2 Major (%) and trace element (10^{-6}) analysis results for the Dalunwusu early-middle Triassic monzogranite and granite porphyry

岩体	GS5215-1	GS5137-1	GS5107-1	TW5127-1	PM54TW7	GS5312-1	GS5312-2
	早三叠世二长花岗岩				中三叠世紫红色花岗斑岩		
SiO ₂	71.80	71.21	71.74	72.71	77.00	77.25	78.08
TiO ₂	0.30	0.32	0.29	0.26	0.08	0.10	0.10
Al ₂ O ₃	15.12	15.05	14.84	14.98	12.27	11.62	11.35
Fe ₂ O ₃	1.40	1.16	1.12	1.36	1.01	0.94	1.02
FeO	0.90	1.47	1.31	0.32	0.49	1.13	0.80
CaO	1.85	2.07	1.72	1.39	0.72	0.60	0.54
MgO	0.69	0.84	0.66	0.60	0.14	0.19	0.15
K ₂ O	3.66	3.25	4.16	4.50	5.11	5.89	5.71
Na ₂ O	4.14	4.47	4.05	3.79	3.15	2.23	2.22
MnO	0.04	0.04	0.03	0.02	0.02	0.03	0.02
P ₂ O ₅	0.09	0.11	0.08	0.07	0.01	0.02	0.02
LOI	1.28	0.60	0.82	0.91	0.33	0.25	0.27
TOTAL	99.70	99.66	99.69	100.13	99.88	99.78	99.81
K ₂ O/Na ₂ O	0.89	0.73	1.03	1.19	1.62	2.64	2.58
FeO _t	2.16	2.52	2.33	1.55	1.40	1.97	1.72
A/CNK	1.07	1.03	1.04	1.10	1.02	1.04	1.05
A/NK	1.40	1.38	1.33	1.35	1.14	1.16	1.15
Mg [#]	40.24	41.22	37.47	44.75	17.69	17.19	15.34
R1	2 388	2 316	2 295	2 392	2 771	2 918	3 027
R2	529	558	508	472	324	302	287
Ga	19.6	19.4	19.8	19.7	21.5	18	16.8
Rb	95.5	107	126	168	383	388	403
Sr	395	748	402	487	24.8	65.4	65.2
Y	4.1	5.33	4.54	4.68	4.47	7.42	5.43
Zr	161	153	146	118	81.7	76	72.5
Nb	3.63	3.78	3.46	3.25	14.3	18.4	15.2
Ba	579	727	901	1 056	52.9	127	132
La	14.7	23.3	20.4	18.7	11	11	9.16
Ce	28.5	42.5	37.8	38.9	17.3	19.6	17.6
Pr	3.31	4.8	4.1	3.78	1.54	1.81	1.42
Nd	11.9	17.2	14.5	13.9	4.13	5.65	4.19
Sm	2.02	2.75	2.34	2.47	0.64	0.9	0.66
Eu	0.59	0.79	0.7	0.49	0.084	0.17	0.15
Gd	1.72	2.35	2.04	1.99	0.71	0.97	0.78
Tb	0.21	0.27	0.23	0.22	0.1	0.17	0.12
Dy	0.78	1.08	0.9	1.01	0.53	1	0.7
Ho	0.14	0.19	0.16	0.16	0.11	0.23	0.17
Er	0.44	0.54	0.48	0.43	0.46	0.83	0.63
Tm	0.049	0.072	0.061	0.062	0.082	0.15	0.1
Yb	0.36	0.47	0.41	0.38	0.69	1.15	0.78
Lu	0.059	0.074	0.058	0.059	0.13	0.2	0.13
Hf	4.46	4.19	3.93	3.57	4.15	3.68	3.21
Ta	0.12	0.14	0.099	0.41	0.97	1.67	1.29
Pb	23.7	27.2	22.8	26.4	51.2	31.7	31.9
Th	15.7	17.4	19.3	13.3	39.4	49	38
U	1.45	1.54	0.92	1.29	8.67	7.06	6.72
δEu	0.97	0.95	0.98	0.68	0.38	0.56	0.64
ΣREE	64.78	96.39	84.18	82.55	37.51	43.83	36.59
(La/Yb) _N	29.30	35.58	35.71	35.31	11.44	6.86	8.43
(La/Sm) _N	4.70	5.48	5.63	4.89	11.11	7.90	8.97
10 000×Ga/Al	2.45	2.43	2.52	2.48	3.31	2.93	2.80

4.2 岩石类型

4.2.1 达伦乌苏早三叠世二长花岗岩

达伦乌苏早三叠世二长花岗岩样品 Sr 含量较高(平均为 508×10^{-6}), Y 含量和 Yb 含量较低, 具较高的 Sr/Y 值(88.55~140.34)和 La/Yb 值(40.83~49.76), 弱的 Eu 负异常(δEu 平均值为 0.89)。这些特征暗示熔融时斜长石在源区是不稳定的, 源区熔体与榴辉岩处于平衡, 对应于高压环境(张旗等, 2020), 这种与榴辉岩平衡的熔体形成的岩浆岩多具埃达克岩特征。样品 SiO_2 平均含量 71.87%, MgO 含量为 0.60%~0.84%, 稀土配分曲线呈右倾型, 微量元素相对亏损 Nb、Ta、Ce、P 等高场强元素, 与典型埃达克岩高硅($\text{SiO}_2 \geq 56\%$)、高铝($\text{Al}_2\text{O}_3 \geq 15\%$)、低 $\text{MgO}(< 3\%)$ 、低 Y($< 18 \times 10^{-6}$)、低 Yb($< 1.9 \times 10^{-6}$)和高 Sr 含量(极少 $< 400 \times 10^{-6}$)等地球化学特征一致, 在微量元素判别图解中也均落入埃达克岩区域内(图 7a)(Defant et al., 1990)。埃达克岩形成于高压环境, 可分为与板块的消减作用有关的 O型埃达克岩和与板块的消减作用

无关的 C型埃达克岩(张旗等, 2002, 2020; 熊万宇康等, 2023)。达伦乌苏早三叠世二长花岗岩属高钾钙碱性系列, 相对 O型埃达克岩更富钾, Al_2O_3 含量和 $\text{Mg}^{\#}$ 值相对更低, 其 Y/Yb 值主要变化于 8~15 之间, 与 C型埃达克岩地球化学特征相一致。该埃达克岩体根据 Wang 等(2006)的分类也属与加厚下地壳相关的埃达克岩(图 7b)。样品 $\text{Mg}^{\#}$ 值较低, 为 37.5~44.7, 与加厚下地壳部分熔融的熔体相符(一般小于 45, Rapp et al., 1995)。实验岩石学研究表明埃达克岩的原岩需满足基性、含水条件, 残留相要有石榴子石存在(张旗等, 2002)。综上所述, 达伦乌苏早三叠世二长花岗岩属 C型埃达克岩, 形成于高压环境, 可能为地壳加厚区底部的下地壳中基性麻粒岩部分熔融形成的。

4.2.2 达伦乌苏中三叠世苏花岗斑岩

达伦乌苏中三叠世花岗斑岩呈小岩株产出, 出露面积小, 与 A型花岗岩侵位高、规模小的特征相符(杨玉柱等, 1993)。岩石呈斑状-似斑状结构, 在冷凝

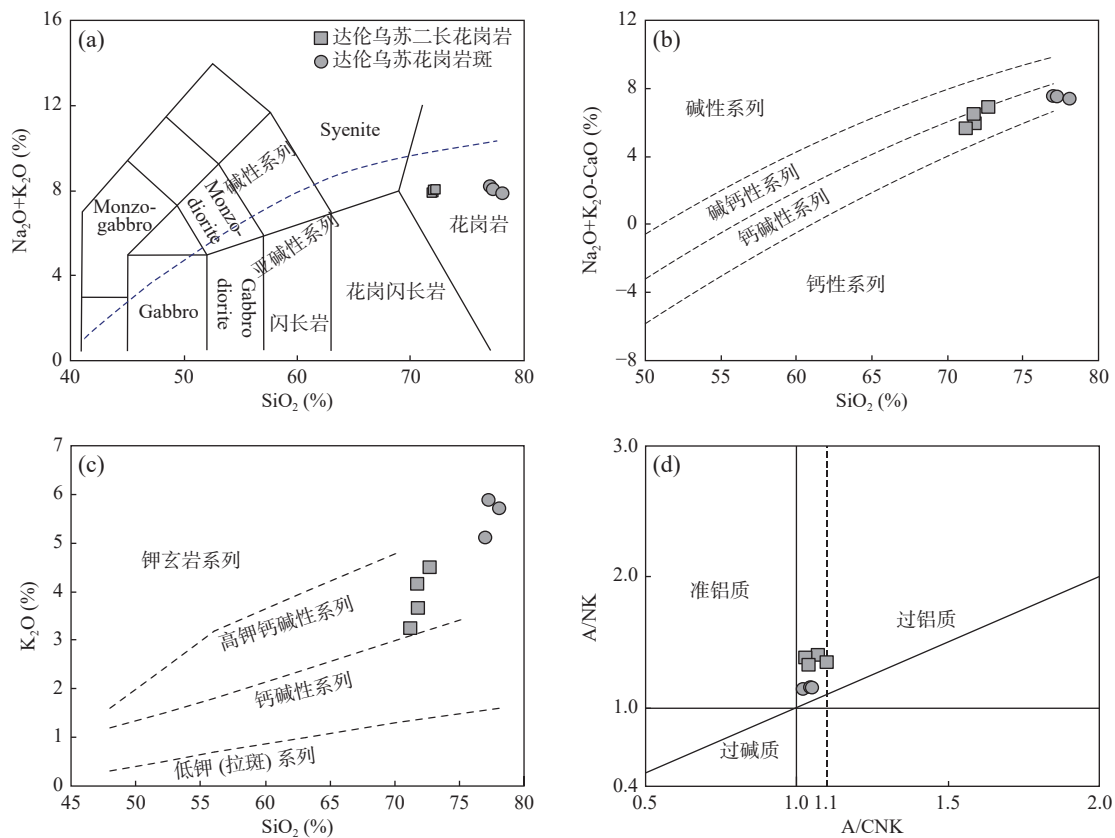
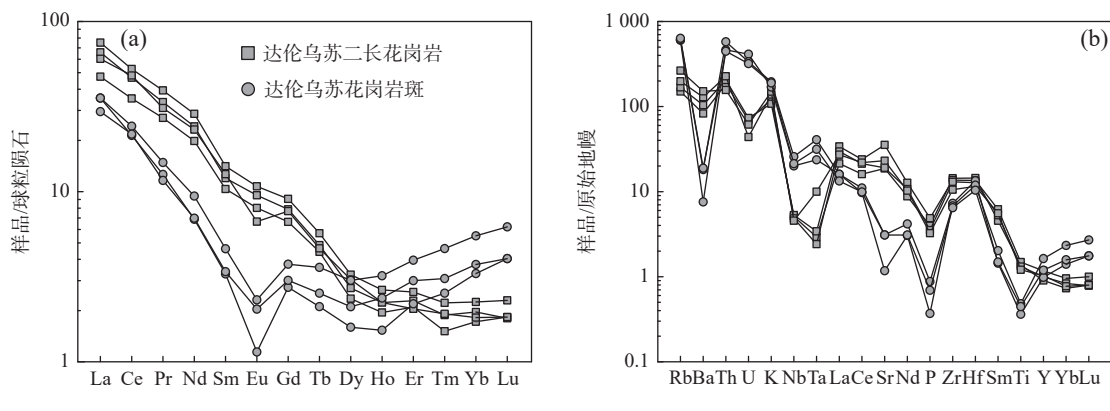


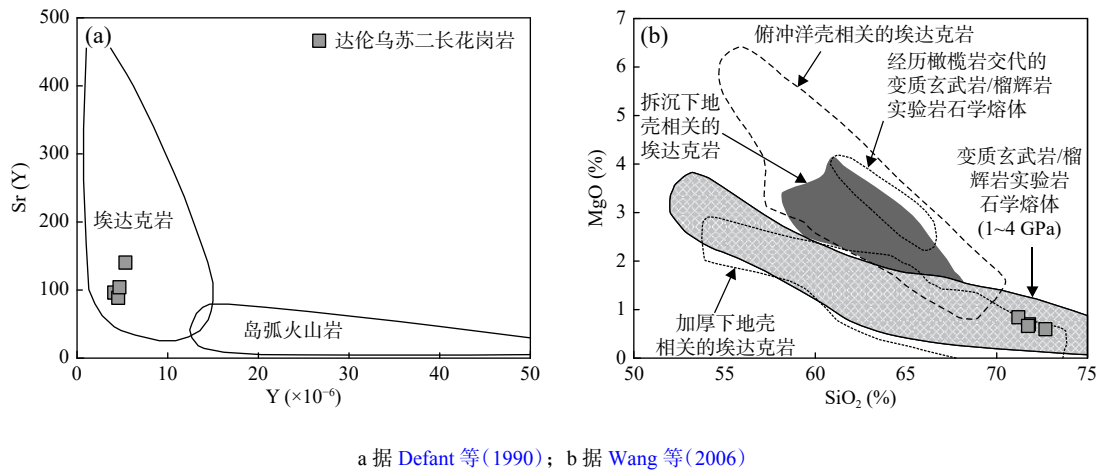
图5 达伦乌苏早三叠世二长花岗岩和花岗斑岩 TAS 图解(a)(据 Middemost, 1994)、 $\text{SiO}_2-(\text{Na}_2\text{O}+\text{K}_2\text{O}-\text{CaO})$ (b)、 $\text{SiO}_2-\text{K}_2\text{O}$ (c) 和 A/NK-A/CNK 图解(d)(据 Miniar et al., 1989)

Fig. 5 (a) TAS diagram, (b) SiO_2 vs. $(\text{Na}_2\text{O} + \text{K}_2\text{O} - \text{CaO})$, (c) SiO_2 vs. K_2O and (d) A/CNK vs. A/NK diagram for the Dalunwusu early Triassic monzogranite and granite porphyry



球粒陨石标准化值据 Boynton (1984); 原始地幔标准化值据 Sun 等(1989)

图6 达伦乌苏早三叠世二长花岗岩和中三叠世花岗斑岩稀土元素球粒陨石标准化配分模式图(a)及微量元素蛛网图(b)
Fig. 6 (a) Chondrite-normalized REE patterns and (b) Primitive mantle-normalized multiple trace element diagrams of the Dalunwusu early-middle Triassic monzogranite and granite porphyry



a 据 Defant 等(1990); b 据 Wang 等(2006)

图7 达伦乌苏早三叠世二长花岗岩岩石类型(a)及构造环境判别图解(b)
Fig. 7 (a) Geochemical classification discrimination and (b) tectonic setting diagrams for Dalunwusu early Triassic monzogranite pluton

过程中仅部分矿物形成了斑晶，暗示岩浆快速上升降温，可能对应于伸展构造环境。化学成分上，样品富SiO₂、富碱、富K，贫CaO、MgO和Al₂O₃，微量元素强烈亏损Ba、Sr、P、Ti，表明源区发生了长石、磷灰石和榍石或金红石的结晶分离作用，与A型花岗岩特征一致(Whalen et al., 1987; Eby, 1992)。因其10 000×Ga/Al值均大于2.6，在Whalen等(1987)的以10 000×Ga/Al值为坐标轴的判别图解中均落入A型花岗岩区域(图8a)。样品具高的FeO/MgO值(9.76~11.58)，属铁质花岗岩，高于长英质I型和S型花岗岩，在Forst等(2001)的主要元素判别图解中也均落入A型花岗岩区域(图8b)。达伦乌苏花岗斑岩具极低的P₂O₅含量(0.01%~0.02%)，与高分异S型花岗岩

(均值为0.14%)不同，具较高的FeO_t含量(1.40%~1.97%)可与高分异I型花岗岩(一般小于1%)区分(贾小辉等, 2009)。样品相对典型A型花岗岩具低的稀土元素含量，δEu值略高(0.38~0.64，一般小于0.3；张旗等, 2012)，但其稀土配分模式图与典型A型花岗岩一致，为“右倾海鸥型”(图6a)，原因可能与源区的稀土元素含量较低有关。本次研究认为达伦乌苏花岗斑岩属A型花岗岩，是低压条件下源岩脱水熔融的产物，形成于伸展构造环境。

4.3 构造意义

珠斯楞-杭乌拉活动大陆边缘近年来发现了较多元古宙地质信息(Wang et al., 2001; Zhang et al., 2016; 宋博等, 2021; 马军等, 2021; 王振义等, 2022)，表明该

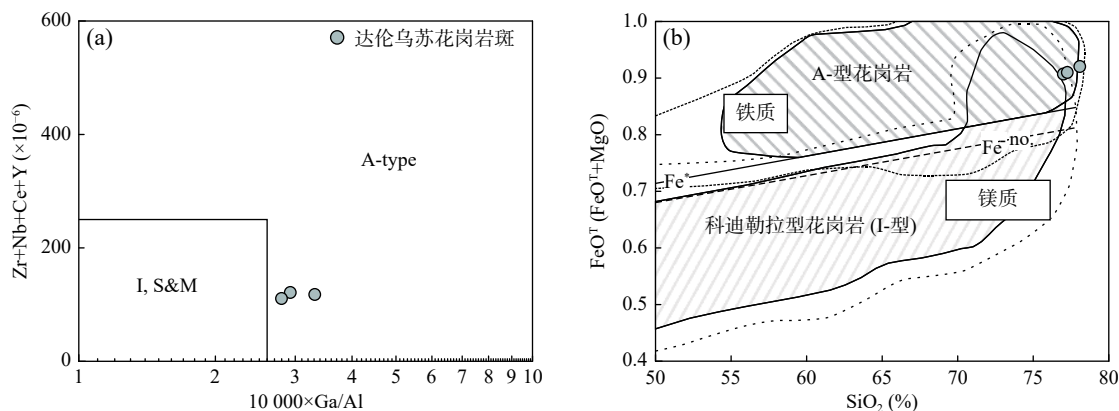


图8 达伦乌苏中三叠世花岗斑岩岩石类型及构造环境判别图解(a据Whalen et al., 1987; b据Forst et al., 2001)

Fig. 8 (a) Geochemical classification and (b) discrimination diagrams of the tectonic setting for Dalunwusu middle Triassic granite porphyry pluton

构造带具前寒武基底,应为蒙古境内划分的南戈壁微陆块的自然延伸。地块北侧圆包山岩浆弧发育有中—下奥陶统咸水湖组和石炭系白山组弧火山岩,分别以为基性火山岩和酸性火山岩为主,反映了奥陶纪—石炭纪火山弧逐渐成熟的过程(吴泰然等,1993;雷聪聪等,2023)。Liu等(2018)根据岩浆岩锆石Hf同位素和全岩Nd同位素研究成果认为298~277 Ma区域处于俯冲构造环境,~230 Ma花岗岩为后碰撞构造环境。查干桃勒盖地区发育一套浅海相沉积碎屑岩,含有海百合化石和繁盛于早—中二叠世海相腕足类化石,可能代表了区域最晚闭合的残余海盆或弧后盆地。微陆块南侧恩格尔乌苏和查干础鲁蛇绿岩带代表的古亚洲洋分支洋的闭合发生在早二叠世后(Zheng et al., 2014)。区域地质发育情况表明,奥陶纪—二叠纪,南戈壁微陆块处于南北两侧古亚洲洋分支洋的俯冲作用下,而其后由造山到造山后的伸展的时代未能精确限定。

研究显示,达伦乌苏早三叠世二长花岗岩属C型埃达克岩,其形成构造背景大致有3种:活动陆缘地壳加厚地区,板块碰撞导致的地壳加厚地区和高原底部,与高压背景有关(张旗等,2002,2003,2020)。该期岩体与中亚造山带东西两段报道的埃达克岩的形成时代相近(谢春林等,2009; Li et al., 2012, 2013, 2017; Wang et al., 2020; Zheng et al., 2020, 2021; Luan et al., 2022)。达伦乌苏中三叠世花岗斑岩属A型花岗岩,可形成于大陆裂谷或板内的非造山环境和与陆-陆碰撞或岛弧岩浆作用有关的后造山环境,均与伸展的构造背景有关(Eby, 1992)。两期构造环境截然不同的岩浆活动共同限定中亚造山带中段南缘由挤压-伸展

的转换时代应在249~241 Ma之间。结合其位于南戈壁微陆块和圆包山岩浆弧之间的活动陆缘区,埃达克岩可能形成于造山晚期的地壳增厚阶段,而A型花岗斑岩应形成于造山后的伸展阶段。这一过程与张旗等(2002)提出的中国东部埃达克岩及其后的拆沉作用模型类似,随着埃达克岩从下地壳大量熔出,下地壳密度增加,导致拆沉作用,形成了A型花岗岩。

5 结论

(1)达伦乌苏二长花岗岩、花岗斑岩岩体分别形成于(249.0±2.3) Ma和(241.0±2.8) Ma,为早—中三叠世岩体。

(2)达伦乌苏早三叠世二长花岗岩具C型埃达克岩地球化学特征,中三叠世花岗斑岩具A型花岗岩地球化学特征。

(3)达伦乌苏早三叠世二长花岗岩具埃达克特征,指示了古亚洲洋闭合后陆壳碰撞加厚的背景,而达伦乌苏中三叠世A型花岗岩指示了造山后伸展构造背景。两期岩浆作用标志着中亚造山带中段南缘在早—中三叠世发生了由增生造山到造山后伸展的构造环境转换。

致谢:匿名审稿人专业的意见建议极大地提高了本文的质量,在此致以诚挚的感谢。

参考文献(References):

陈井胜,刘正宏,刘永江,等.中亚造山带东段构造演化研究进展:前言[J].*岩石学报*,2022,38(8):2175–2180.

- CHEN Jingsheng, LIU Zhenghong, LIU Yongjiang, et al. Recent Progress in the evolution of eastern segment of the Central Asia Orogenic Belt[J]. *Acta Petrologica Sinica*, 2022, 38(8): 2175–2180.
- 董玉, 王德森, 于倩, 等. 中国东北地区晚古生代构造-岩浆演化历史[J]. *岩石学报*, 2022, 38(8): 2249–2268.
- DONG Yu, WANG Simiao, YU Qian, et al. Late Paleozoic tectonic-magmatic evolution history of the northeastern China[J]. *Acta Petrologica Sinica*, 2022, 38(8): 2249–2268.
- 付超, 李俊建, 张帅, 等. 中蒙边界地区侵入岩时空分布特征及对构造演化的启示[J]. *华北地质*, 2023, 46(1): 1–19.
- FU Chao, LI Junjian, ZHANG Shuai, et al. The temporal and spatial distribution characteristics of intrusive rocks in the border area between China and Mongolia and its implications for tectonic evolution[J]. *North China Geology*, 2023, 46(1): 1–19.
- 贾小辉, 王强, 唐功建. A型花岗岩的研究进展及意义[J]. *大地构造与成矿学*, 2009, 33(3): 465–480.
- JIA Xiaohui, WANG Qiang, TANG Gongjian. A-type Granites: Research Progress and Implications[J]. *Geotectonica et Metallogenesis*, 33(3), 2009, 33(3): 465–480.
- 雷聪聪, 薄海军, 丁海生, 等. 内蒙古自治区雅干地区白山组火山岩 LA-ICP-MS 锆石 U-Pb 年龄及其构造环境[J]. *地质通报*, 2023, 42(12): 2096–2108.
- LEI Congcong, BO Haijun, DING Haisheng, et al. LA-ICP-MS zircon U-Pb dating and tectonic setting of volcanic rocks of Baishan Formation in Yagan area, Inner Mongolia Autonomous Region[J]. *Geological Bulletin*, 2023, 42(12): 2096–2108.
- 李凤春, 侯明兰, 栾日坚, 等. 电感耦合等离子体质谱仪与激光器联用测量条件优化及其在锆石 U-Pb 定年中的应用[J]. *岩矿测试*, 2016, 35(1): 17–23.
- LI Fengchun, HOU Minglan, LUAN Rijian, et al. Optimization of Analytical Conditions for LA-ICP-MS and Its Application to Zircon U-Pb Dating[J]. *Rock and Mineral Analysis*, 2016, 35(1): 17–23.
- 刘桂萍, 郭瑞清, 魏震, 等. 新疆库鲁克塔格地区古生代花岗质侵入岩全岩 Sr-Nd 和锆石 Hf 同位素地球化学特征及其意义[J]. *西北地质*, 2021, 54(3): 39–50.
- LIU Guiping, GUO Ruiqing, WEI Zhen, et al. Geochemical Characteristics and Significance of the Whole Rock Sr-Nd and Zircon Hf Isotopic in the Paleozoic Granite-plutons in Kuruktag, Xinjiang[J]. *Northwestern Geology*, 2021, 54(3): 39–50.
- 刘基, 王丕军, 薄海军. 内蒙古额济纳旗内乔伦恩格次黑云母二长花岗斑岩中锆石的特征及其指示意义[J]. *西北地质*, 2020, 53(3): 41–55.
- LIU Ji, WANG Pijun, BO Haijun. Characteristics and Implications of Zircon in Qiaolun'en'geci Biotite Monzogranite Porphyry in Ejina County, Inner Mongolia[J]. *Northwestern Geology*, 2020, 53(3): 41–55.
- 马军, 雷聪聪, 王文宝, 等. 阿拉善地块北缘雅干地块诸小布和糜棱岩化花岗岩地球化学特征、锆石 U-Pb 年龄及构造背景研究[J]. *矿物岩石地球化学通报*, 2021, 40(6): 1357–1368.
- MA Jun, LEI Congcong, WANG Wenbao, et al. A Study on Geochemistry, Zircon U-Pb Dating and Tectonic Setting of the Zhuxiaobuhe Mylonitized Granite in the Yagan Area of Northern Margin of the Alxa Terrain[J]. *Bulletin of Mineralogy, Petrology and Geochemistry*, 2021, 40(6): 1357–1368.
- 邵积东. 内蒙古地质构造单元划分及存在的有关问题[J]. *西部资源*, 2016, 3: 84–87+150.
- SHAO Jidong. Division of geological tectonic units of Inner Mongolia and related problems[J]. *Westrn Resources*, 2016, 3: 84–87+150.
- 邵济安, 唐克东, 何国琦. 内蒙古早二叠世构造古地理的再造[J]. *岩石学报*, 2014, 30(7): 1858–1866.
- SHAO Jian, TANG Kedong, HE Guoqi. Early Permian tectono-palaeogeographic reconstruction of Inner Mongolia, China[J]. *Acta Petrologica Sinica*, 2014, 30(7): 1858–1866.
- 舍建忠, 贾健, 金成, 等. 西准噶尔谢米斯台山中段晚石炭世 A 型花岗岩地球化学特征及岩石成因[J]. *地质通报*, 2023, 42(7): 1051–1068.
- SHE Jianzhong, JIA Jian, JIN Cheng, et al. Geochemical characteristics and petrogenesis of Late Carboniferous A-type granites in the middle section of Xiemisitai Mountain, West Junggar[J]. *Geological Bulletin of China*, 2023, 42(7): 1051–1068.
- 宋博, 张慧元, 魏东涛, 等. 中亚造山带南缘中-新元古代地壳的揭示——来自北山-阿拉善北部钻遇碱性花岗岩的年代学和 Hf 同位素示踪研究[J]. *地球学报*, 2021, 42(1): 9–20.
- SONG Bo, ZHANG Huiyuan, WEI Dongtao, et al. Revelation of the Meso -Neoproterozoic Crust on the Southern Margin of the Central Asian Orogenic Belt: Chronology and Hf Isotope Tracer from Drilling-intersected Alkaline Granites, Northern Beishan-Alxa[J]. *Acta Geoscientica Sinica*, 2021, 42(1): 9–20.
- 王丕军. 额济纳旗乔伦恩格次花岗岩特征及构造环境研究[D]. 北京: 中国地质大学(北京), 2018.
- WANG Pijun. Characteristics and Tectonic Environment of Qiaolun'en'geci Granite in Ejina County[D]. Beijing: China University of Geosciences(Beijing), 2018.
- 王廷印, 王金荣, 王士政, 等. 华北板块和塔里木板块之关系[J]. *地质学报*, 1993, 67(4): 287–300.
- WANG Tingyin, WANG Jinrong, WANG Shizheng, et al. Relationships between the North China and Tarim Plates[J]. *Acta Geologica Sinica*, 1993, 67(4): 287–300.
- 王元元, 杨小强, 阿种明, 等. 新疆西准噶尔沙勒克腾地区花岗岩锆石 U-Pb 年龄、地球化学特征及其对后碰撞构造环境的约束[J]. *地质通报*, 2023, 42(4): 600–615.
- WANG Yuanyuan, YANG Xiaoqiang, A Zhongming, et al. Zircon U-

- Pb age, geochemistry of granites in Shaleketeng area, West Junggar, Xinjiang and its constraints on the post-collision tectonic environment[J]. *Geological Bulletin of China*, 2023, 42(4): 600–615.
- 王振义, 李钢柱, 丁海生, 等. 内蒙古额济纳旗雅干地区北山岩群的厘定及其地质意义[J]. *地球科学*, 2022, 47(4): 1177–1193.
- WANG Zhenyi, LI Gangzhu, DING Haisheng, et al. Determination and Geological Significance of Beishan Group in Yagan Area, Ejiana, Inner Mongolia[J]. *Earth Science*, 2022, 47(4): 1177–1193.
- 吴泰然, 何国琦. 内蒙古阿拉善地块北缘的构造单元划分及各单元的基本特征[J]. *地质学报*, 1993, 67(2): 97–108.
- WU Tairan, HE Guoqi. Tectonic units and their fundamental characteristics on the northern margin of the Alxa Block[J]. *Acta Geologica Sinica*, 1993, 67(2): 97–108.
- 谢春林, 杨建国, 王立社, 等. 甘肃北山地区古亚洲南缘古生代岛弧带位置的讨论[J]. *地质学报*, 2009, 83(11): 1584–1599.
- XIE Chunlin, YANG Jianguo, WANG Lishe, et al. Discussion on the Location of Paleozoic Island Arc Zone on the South Margin of Paleo-Asian Ocean in the Beishan Area of Gansu Province[J]. *Acta Geologica Sinica*, 2009, 83(11): 1584–1599.
- 辛后田, 牛文超, 田健, 等. 内蒙古北山造山带时空结构与古亚洲洋演化[J]. *地质通报*, 2020, 39(9): 1297–1316.
- XIN Houtian, NIU Wenchao, TIAN Jian, et al. Spatio-temporal structure of Beishan orogenic belt and evolution of Paleo-Asian Ocean, Inner Mongolia[J]. *Geological Bulletin of China*, 2020, 39(9): 1297–1316.
- 熊万宇康, 赵梦琪, 于森, 等. 造山带洋陆转换过程与岩浆作用: 以东昆仑都兰地区古生代花岗岩为例[J]. *西北地质*, 2023, 56(6): 113–139.
- XIONG Wanyukang, ZHAO Mengqi, YU Sen, et al. Ocean–Continent Transition Process and Magmatism in Orogenic Belts: A Case Study of Paleozoic Granites in the Dulan Area of East Kunlun[J]. *Northwestern Geology*, 2023, 56(6): 113–139.
- 杨玉柱, 袁万明. A型花岗岩的鉴别标志[J]. *河北地质学院学报*, 1993, 16(2): 150–158.
- YANG Yuzhu, YUAN Wanming. Discriminating Marks of A-type Granitoids[J]. *Journal of Hebei College of Geology*, 1993, 16(2): 150–158.
- 张旗, 焦守涛. 埃达克岩来自高压背景——一个科学的、可靠的、有预见性的科学发现[J]. *岩石学报*, 2020, 36(6): 1675–1683.
- ZHANG Qi, JIAO Shoutao. Adakite comes from a high-pressure background: A scientific, reliable, predictable scientific discovery[J]. *Acta Petrologica Sinica*, 2020, 36(6): 1675–1683.
- 张旗, 冉皞, 李承东. A型花岗岩的实质是什么?[J]. *岩石矿物学杂志*, 2012, 31(4): 621–626.
- ZHANG Qi, RAN Hao, LI Chengdong. A-type granite: what is the essence?[J]. *Acta Petrologica et Mineralogica*, 2012, 31(4): 621–626.
- 张旗, 王焰, 刘伟, 等. 埃达克岩的特征及其意义[J]. *地质通报*, 2002, 21(7): 431–435.
- ZHANG Qi, WANG Yan, LIU Wei, et al. Adakite: Its characteristics and implications[J]. *Geological Bulletin of China*, 2002, 21(7): 431–435.
- 张旗, 王焰, 王元龙. 埃达克岩与构造环境[J]. *大地构造与成矿学*, 2003, 27(2): 101–108.
- ZHANG Qi, WANG Yan, WANG Yuanlong. On the relationship between adakite and its tectonic setting[J]. *Geotectonica et Metallogenesis*, 2003, 27(2): 101–108.
- 张永玲, 张治国, 刘希军, 等. 内蒙朝克山辉长岩中单斜辉石矿物化学特征及地质意义[J]. *西北地质*, 2024, 57(1): 122–138.
- ZHANG Yongling, ZHANG Zhiguo, LIU Xijun, et al. Mineralogical Chemistry Characteristics and Geological Significance of the Clinopyroxene from Chaokeshan Gabbro, Inner Mongolia[J]. *Northwestern Geology*, 2024, 57(1): 122–138.
- 郑荣国, 吴泰然, 张文, 等. 阿拉善地块北缘雅干花岗岩体地球化学、地质年代学及其对区域构造演化制约[J]. *岩石学报*, 2013, 29(8): 2665–2675.
- ZHENG Rongguo, WU Tairan, ZHANG Wen, et al. Geochronology and geochemistry of the Yagan granite in the northern margin of the Alxa block: Constraints on the tectonic evolution of the southern Altaiids[J]. *Acta Petrologica Sinica*, 2013, 29(8): 2665–2675.
- Badarch G, Cunningham W D, Windley B F. A new terrane subdivision for Mongolia: implications for the Phanerozoic crustal growth of Central Asia[J]. *Journal of Asian Earth Sciences*, 2002, 21(1): 87–110.
- Boynton W V. Geochemistry of the rare earth elements: meteorite studies[A]. In Henderson P (ed.). *Rare earth element geochemistry*[M]. Amsterdam, Elsevier, 1984: 63–114.
- Charvet J, SHU Liangshu, Laurent-Charvet S. Paleozoic structural and geodynamic evolution of eastern Tianshan (NW China): welding of the Tarim and Junggar plates[J]. *Episodes*, 2007, 30: 162–186.
- Defant M J, Drummond M S. Derivation of Some Modern Arc Magmas by Melting of Young Subducted Lithosphere[J]. *Nature*, 1990, 347(6294): 662–665.
- Du Long, Long Xiaoping, Yuan Chao, et al. Petrogenesis of Late Paleozoic diorites and A-type granites in the central Eastern Tianshan, NW China: Response to post-collisional extension triggered by slab breakoff[J]. *Lithos*, 2018, 318: 47–59.
- Eby G N. Chemical subdivision of the A-type granitoids: petrogenetic

- ic and tectonic implications[J]. *Geology*, 1992, 20(7): 641–644.
- Eizenhöfer P R, ZHAO Guochun. Solonker Suture in East Asia and its bearing on the final closure of the eastern segment of the Palaeo-Asian Ocean[J]. *Earth-Science Reviews*, 2018, 186: 153–172.
- Forst B R, Barnes C G, Collins W J, et al. A Geochemitic Classification For Granitic Rocks[J]. *Journal of Petrology*, 2001, 42(11): 2033–2042.
- Fu Dong, Huang Bo, Kusky T M, et al. A middle Permian ophiolitic mélangé belt in the Solonker suture zone, western Inner Mongolia, China: Implications for the evolution of the Paleo-Asian Ocean[J]. *Tectonics*, 2018, 37: 1292–1320.
- Jian Ping, Kröner A, Jahn B M, et al. Zircon dating of Neoproterozoic and Cambrian ophiolites in West Mongolia and implications for the timing of orogenic processes in the central part of the Central Asian Orogenic Belt[J]. *Earth-Science Reviews*, 2014, 133: 62–93.
- Jian Ping, LIU Dunyi, Kröner A, et al. Time scale of an early to mid-Paleozoic orogenic cycle of the long-lived Central Asian Orogenic Belt, Inner Mongolia of China: Implications for continental growth[J]. *Lithos*, 2008, 101: 233–259.
- Li HaoDong, Zhou JianBo, Wilde S A. Nature and development of the South Tianshan-Solonker suture zone[J]. *Earth-Science Reviews*, 2022, 223: 104189.
- Li Jinyi. Permian geodynamic setting of Northeast China and adjacent regions: closure of the Paleo-Asian Ocean and subduction of the Paleo-Pacific Plate[J]. *Journal of Asian Earth Sciences*, 2006, 26(3–4): 207–224.
- Li Shan, Chung S L, Wilde S A, et al. Early - Middle Triassic high Sr/Y granitoids in the southern Central Asian Orogenic Belt: Implications for ocean closure in accretionary orogens[J]. *Journal of Geophysical Research: Solid Earth*, 2017, 122(3): 2291–2309.
- Li Shan, Wang Tao, Wilde S A, et al. Geochronology, petrogenesis and tectonic implications of Triassic granitoids from Beishan, NW China[J]. *Lithos*, 2012, 134–135: 123–145.
- Li Shan, Wang Tao, Wilde S A, et al. Evolution, source and tectonic significance of Early Mesozoic granitoid magmatism in the Central Asian Orogenic Belt (central segment). *Earth-Science Reviews*[J], 2013, 126: 206–234.
- Liu Min, Lai Shacong, Zhang Da, et al. Middle Permian high Sr/Y monzogranites in central Inner Mongolia: reworking of the juvenile lower crust of Bainaimiao arc belt during slab break-off of the Palaeo-Asian oceanic lithosphere[J]. *International Geology Review*, 2019, 61(17): 2083–2099.
- Liu Qian, Zhao Guochun, Han Yigui, et al. Early Paleozoic subduction processes of the Paleo-Asian Ocean: insights from geochronology and geochemistry of Paleozoic plutons in the Alxa Terrane[J]. *Lithos*, 2016, 262: 546–560.
- Liu Qian, Zhao Guochun, Han Yigui, et al. Timing of the final closure of the Paleo-Asian Ocean in the Alxa Terrane: Constraints from geochronology and geochemistry of Late Carboniferous to Permian gabbros and diorites[J]. *Lithos*, 2017, 274–275: 19–30.
- Liu Qian, Zhao Guochun, Han Yigui, et al. Geochronology and geochemistry of Paleozoic to Mesozoic granitoids in western Inner Mongolia, China: implications for the tectonic evolution of the southern Central Asian Orogenic Belt[J]. *The Journal of Geology*, 2018, 126(4): 451–471.
- Liu Yongsheng, Wang Xiaohong, Wang Dongbing, et al. Triassic high-Mg adakitic andesites from Linxi, Inner Mongolia: insights into the fate of the Paleo-Asian ocean crust and fossil slab-derived melt-peridotite interaction[J]. *Chemical Geology*, 2012, 328: 89–108.
- Lu Jia, Zhang Chen, Liu Dongdong. Geochronological, geochemical and Sr-Nd-Hf isotopic studies of the A-type granites and adakitic granodiorites in Western Junggar: Petrogenesis and tectonic implications[J]. *Minerals*, 2020, 10(397): 1–25.
- Ludwig K R. Isoplot 3.00: A Geochronological Toolkit for Microsoft Excel[CP]. Berkeley: Berkeley Geochronology Center. 2003.
- Luan JinPeng, Tang Jie, et al. Accretion kinematics and driving mechanism of the eastern Central Asian Orogenic Belt: Insights from seismic tomography and middle Permian-Middle Triassic magmatism in central Jilin Province[J]. *Gondwana Research*, 2022, 101: 114–131.
- Middemost E A K. Naming materials in the magma/igneous rock system[J]. *Earth-Science Reviews*, 1994, 37(3–4): 215–224.
- Miniar P D, Piccoli P M. Tectonic discrimination of granitoids[J]. *Geological Society of America Bulletin*, 1989, 101(5): 635–643.
- Rapp R P, Watson E B. Dehydration Melting of Metabasalt at 8–32 kbar: Implications for Continental Growth and Crust Mantle Recycling[J]. *Journal of Petrology*, 1995, 36(4): 891–931.
- Sengör A M C, Natal'in B A, Burtman V S. Evolution of the Altaiid tectonic collage and Palaeozoic crustal growth in Eurasia[J]. *Nature*, 1993, 364(6435): 299–307.
- Shi Guanghai, Miao Laicheng, Zhang Fuqing, et al. Emplacement age and tectonic implications of the Xilinhhot A-type granite in Inner Mongolia, China[J]. *Chinese Science Bulletin*, 2004, 49(7): 723–729.
- Shi Yuruo, Anderson J L, Li Linlin, et al. Zircon ages and Hf isotopic compositions of Permian and Triassic A-type granites from central Inner Mongolia and their significance for late Palaeozoic and early Mesozoic evolution of the Central Asian Orogenic

- Belt[J]. *International Geology Review*, 2016, 58(8): 967–982.
- Song Dongfang, Xiao Wenjiao, Windley B F, et al. Carboniferous to Early Triassic magmatism and accretion in Alxa(NW China): implications for accretionary orogenesis of the southern Altaiids[J]. *Journal of the Geological Society*, 2020, 177: 997–1012.
- Sun S S, McDonough W F. Chemical and isotopic systematics of oceanic basalts: implications for mantle composition and processes[J]. *Geological Society, London, Special Publications*, 1989, 42(1): 313–345.
- Wang Qiang, Xu Jifeng, et al. Petrogenesis of Adakitic Porphyries in an Extensional Tectonic Setting, Dexing, SouthChina: Implications for the Genesis of Porphyry Copper Mineralization[J]. *Journal of Petrology*, 2006, 47(1): 119–144.
- Wang Tao, Tong Ying, Xiao Wenjiao, et al. Rollback, scissor-like closure of the Mongol-Okhotsk Ocean and formation of an orocline: magmatic migration based on a large archive of age data[J]. *National science review*, 2022, 9(5): nwab210.
- Wang Tao, Zheng Yadong, Gehrels G E, et al. Geochronological evidence for existence of South Mongolian microcontinent—A zircon U-Pb age of grantoid gneisses from the Yagan-Onch Hayrhan metamorphic core complex[J]. *Chinese Science Bulletin*, 2001, 46(23): 2005–2008.
- Wang Wenlong, Teng Xuejian, Liu Yang, et al. From subduction to post - collision: Early Permian - middle Triassic magmatic records from Langshan Belt, Central Asian Orogenic Belt[J]. *Geological Journal*, 2020, 55(3): 2167–2184.
- Whalen J B, Currie K L, Chappell B W. A-type granites: geochemical characteristics, discrimination and petrogenesis[J]. *Contributions to Mineralogy and Petrology*, 1987, 95: 407–419.
- Windley B F, Alexeiev D, XIAO Wenjiao, et al. Tectonic models for accretion of the Central Asian Orogenic Belt[J]. *Journal of the Geological Society*, 2007, 164(1): 31–47.
- Wu Fuyuan, Sun Deyou, Li Huimin , et al, A-type granites in North-eastern China: age and geochemical constraints on their petrogenesis[J]. *Chemical Geology*, 2002, 187, 143–173.
- Xiao Wenjiao, Windley B F, Han Chunming, et al. Late Paleozoic to early Triassic multiple roll-back and oroclinal bending of the Mongolia collage in Central Asia[J]. *Earth-Science Reviews*, 2018, 186: 94–128.
- Xiao Wenjiao, Windley B F, Hao Jie, et al. Accretion leading to collision and the Permian Solonker suture, Inner Mongolia, China: Termination of the central Asian orogenic belt[J]. *Tectonics*, 2003, 22(6): 1069.
- Xu Bei, Charvet J, Chen Yan, et al. Middle Paleozoic convergent orogenic belts in western Inner Mongolia (China): framework, kinematics, geochronology and implications for tectonic evolution of the Central Asian Orogenic Belt[J]. *Gondwana Research*, 2013, 23(4): 1342–1364.
- Yan Quanshu, Metcalfe I, Shi Xuefa, et al. Early Cretaceous granitic rocks from the southern Jiaodong Peninsula, eastern China: implications for lithospheric extension[J]. *International Geology Review*, 2019, 61(7): 821–838.
- Zhang Wen, Pease V, Meng Qingpeng, et al. Discovery of a Neoproterozoic granite in the Northern Alxa region, NW China: its age, petrogenesis and tectonic significance[J]. *Geological Magazine*, 2016, 153(03): 512–523.
- Zheng Jiahao, Mao Jingwen, Chai Fengmei, et al. Petrogenesis of Permian A-type granitoids in the Cihai iron ore district, Eastern Tianshan, NW China: Constraints on the timing of iron mineralization and implications for a non-plume tectonic setting[J]. *Lithos*, 2016, 260: 371–383.
- Zheng Rongguo, Li Jinyi, Zhang Jin, et al. Permian oceanic slab subduction in the southmost of Central Asian Orogenic Belt: Evidence from adakite and high-Mg diorite in the southern Beishan[J]. *Lithos*, 2020, 358: 105406.
- Zheng Rongguo, Li Jinyi, Zhang Jin, et al. A prolonged subduction-accretion in the southern Central Asian Orogenic Belt: Insights from anatomy and tectonic affinity for the Beishan complex[J]. *Gondwana Research*, 2021, 95: 88–112.
- Zheng Rongguo, Wu Tairan, Zhang Wen, et al. Late Paleozoic subduction system in the northern margin of the Alxa block, Altaiids: geochronological and geochemical evidences from ophiolites[J]. *Gondwana Research*, 2014, 25(2): 842–858.